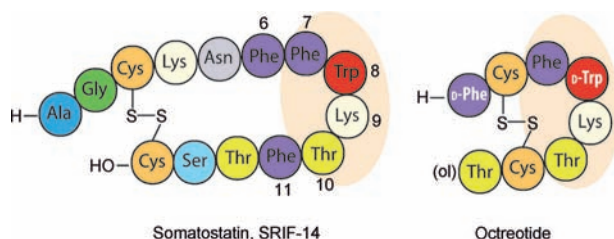


# Fine-tuning the $\pi$ - $\pi$ Aromatic Interactions in Peptides: Somatostatin Analogues Containing Mesityl Alanine\*\*

Pablo Martín-Gago, Marc Gomez-Caminals, Rosario Ramón, Xavier Verdaguer, Pau Martin-Malpartida, Eric Aragón, Jimena Fernández-Carneado, Berta Ponsati, Pilar López-Ruiz, Maria Alicia Cortes, Begoña Colás, Maria J. Macias,\* and Antoni Riera\*

Understanding noncovalent interactions between aromatic moieties is essential in medicinal chemistry and lead optimization for drug design. These interactions are fundamental in controlling diverse phenomena; for example, vertical stacking interactions provide stability to duplex DNA.<sup>[1]</sup> Other important examples include the spike-nucleocapsid interaction in viruses,<sup>[2a]</sup> molecular self-assembly in supramolecular systems,<sup>[2b]</sup> and host-guest molecular recognition events.<sup>[2c]</sup> Aromatic amino acids strongly contribute to protein architecture and stability<sup>[3,4]</sup> as it has been observed in SH3 and WW domains,<sup>[5a]</sup> and of peptides, including the antimicrobial Tachiplesin I<sup>[5b]</sup> or the pharmacologically important hormone somatostatin.<sup>[6]</sup>

Somatostatin, also known as somatotropin release-inhibiting factor (SRIF), is a 14-amino-acid natural peptide whose sequence is shown in Figure 1 (left). In clinical practice, somatostatin is currently used as a gastric anti-secretory drug to treat growth hormone secretion disorders and endocrine tumors.<sup>[7]</sup> It is involved in multiple biological functions mediated by direct interactions between it and at least five characterized G-protein-coupled receptors, named SSTR1–5.<sup>[8]</sup> These receptors differ in their tissue distribution and pharmacological properties.



**Figure 1.** Amino acid sequences of somatostatin and octreotide, and their respective proposed pharmacophores.

The three-dimensional (3D) structure of somatostatin has been a matter of debate during the last three decades. Initially, Hirschmann and co-workers<sup>[9]</sup> postulated the existence of an interaction between the aromatic residues Phe6 and Phe11. This interaction could enable in the stabilization of some of the biologically active conformations of the hormone. A few years later, the same authors detected the Phe6–Phe11 interaction by NMR spectroscopy,<sup>[10a]</sup> and hypothesized that it should be perpendicular (edge-to-face) rather than parallel (face-to-face).<sup>[10a,b]</sup> However, van Binst and co-workers subsequently reported that they were unable to observe the Phe6–Phe11 interaction by NMR spectroscopy (either in aqueous solution or in methanol) and that the only interaction that they could observe was that between Phe6 and Phe7.<sup>[11a,b]</sup> Attempts to additionally characterize the somatostatin structure have been unsuccessful. Presently, there is a consensus that the native structure of somatostatin in solution is an ensemble of several conformations in equilibrium, a few of which are partially structured.<sup>[12]</sup> This scenario probably explains the failure to obtain detailed NMR or X-ray data on the 3D structure of the peptide.

To date, most of the work done on somatostatin analogues has focused on the synthesis of molecules having smaller and more rigid rings. Some of these compounds have shown enhanced selectivity and stability.<sup>[13]</sup> The best examples are octreotide (Figure 1, right) and lanreotide, the only two somatostatin analogue drugs on the market.<sup>[14]</sup> Both of these compounds have strong affinity for SSTR2 but only moderate to low affinity for the other receptors. Like most of the somatostatin analogues currently under research, octreotide and lanreotide are octapeptides that include part of the somatostatin pharmacophore<sup>[15]</sup> and feature a covalent disulfide bridge as a surrogate of the proposed noncovalent interaction between Phe6 and Phe11.

[\*] P. Martín-Gago, Dr. R. Ramón, Prof. X. Verdaguer, P. Martin-Malpartida, E. Aragón, Prof. M. J. Macias, Prof. A. Riera Institute for Research in Biomedicine (IRB Barcelona) Baldori Reixac, 10, 08028 Barcelona (Spain) E-mail: antoni.riera@irbbarcelona.org maria.macias@irbbarcelona.org

Dr. R. Ramón, Prof. X. Verdaguer, Prof. A. Riera Departament de Química Orgànica, Universitat de Barcelona Martí i Franqués, 1–11, 08028 Barcelona (Spain)

Prof. M. J. Macias Institució Catalana de Recerca i Estudis Avançats (ICREA) Passeig Lluís Companys 23, Barcelona (Spain)

Dr. M. Gomez-Caminals, Dr. J. Fernández-Carneado, Dr. B. Ponsati BCN Peptides, S.A. (Lipotec Group) Barcelona (Spain)

Prof. P. López-Ruiz, M. A. Cortes, Prof. B. Colás Departamento de Bioquímica y Biología Molecular, Universidad de Alcalá de Henares, Facultad de Medicina, Madrid (Spain)

[\*\*] We thank the MICINN (CTQ2008-00763/BQU and BFU2008-02795), IRB Barcelona, the Generalitat de Catalunya (2009SGR 00901), and BCN Peptides S.A. for financial support. R.R. and P.M.-G. thank the MICINN for a doctoral fellowship. E.A. and M.J.M. thank the Consolider RNAREG (CSD2009-00080) for financial support.

Supporting information for this article is available on the WWW under <http://dx.doi.org/10.1002/anie.201106406>.

Given recent advances in peptide chemistry which have greatly facilitated synthesis of large cyclic peptides, we reasoned that we could introduce point modifications into the 14-residue scaffold to fine-tune rigidity, specificity, and stability to produce new analogues that are structurally much closer to the natural hormone than the octapeptides. In previous studies,<sup>[16]</sup> we explored the substitution of Trp8 with 3-(3'-quinolyl) alanine (Qla, both enantiomers), and found that the corresponding analogues exhibit more conformational variability than does somatostatin itself. Remarkably, these analogues were selective for SSTR1 and SSTR3 receptors. Thus, we deduced that structural flexibility is advantageous for activity in certain receptors and that relative to the parent compound, these Qla analogues have a greater proportion of highly flexible conformers in solution.

In seeking new somatostatin analogues that would be conformationally stabilized (by  $\pi$ - $\pi$  interactions) relative to the parent compound, we substituted key amino acids in somatostatin with nonnatural residues. We prepared various analogues by replacing the aromatic ring of the phenylalanine with a mesityl group (2,4,6-trimethylphenyl), that is, by substituting one Phe with 3-mesityl alanine (Msa, **1**; see Figure 2). We chose Msa based on the higher electronic density that the methyl groups confer upon the aromatic moiety, and on the reduced conformational mobility of the mesityl ring relative to Phe.<sup>[17]</sup> Hence, we expected that the  $\pi$ - $\pi$  interactions between the Msa and the remaining Phe residues would be stronger than those among the Phe groups of the parent compound, and envisaged that the intrinsic rigidity of the Msa amino acid could shift the conformational equilibrium towards more rigid conformations (relative to those of the natural compound).

We initially prepared two different peptides containing Msa instead of Phe at either position 6 or 11. Additionally, to increase the physiological stability of the resulting peptides in blood plasma, we used D-Trp (instead of L-Trp) at position 8 (peptides **2** and **3**; Figure 2), a modification known to enhance stability while maintaining the biological activity of the peptide.<sup>[7a,9,18]</sup> Since the aromatic interaction had been postulated to occur either between residues 6 and 11 (Veber et al.)<sup>[9]</sup> or between residues 6 and 7 (Jans et al.),<sup>[11a]</sup> we were also interested in the effects of substituting Phe7 with Msa (peptide **4**). The resulting analogue exhibited outstanding receptor affinity, which prompted us to study the effects of D-Trp substitution in this compound; thus, we prepared the same sequence with L-Trp8 (peptide **5**).

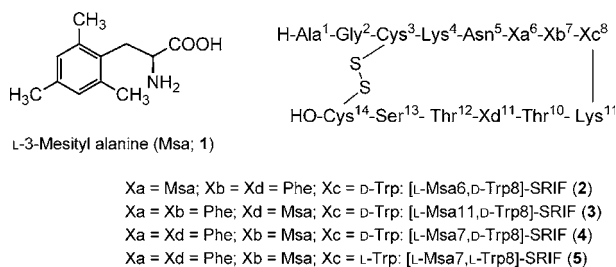
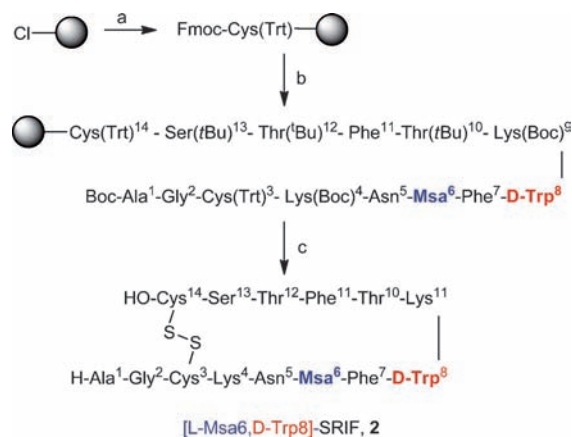


**Figure 2.** The new somatostatin analogues **2–5** having L-3-mesityl alanine (Msa).

Herein we present how the structural studies confirmed that the aromatic interactions do exist, and significantly contribute to both the greater stability and structural rigidity of our peptide analogues relative to somatostatin. Moreover, we have also evaluated the interaction of these derivatives with the five receptors in cellular cultures. We have found that each of these peptides exhibits a unique profile of strong affinity and selectivity for one or more of the receptors SSTR1–5. Furthermore, we have correlated this selectivity to the presence of aromatic clusters on the basis of the NMR data, thus paving the way for a rational design of new efficacious somatostatin-based analogues. We have also characterized the relative orientation of the aromatic rings in the clusters, and found that each peptide displays a particular  $\pi$ - $\pi$  interaction fingerprint, including parallel, offset-stacked, and perpendicular orientations as has been described for proteins.<sup>[3]</sup>

We obtained Fmoc-L-3-mesityl alanine by following a procedure previously developed by our group.<sup>[19]</sup> The four peptides containing Msa, at either position 6 [L-Msa6,D-Trp8]-SRIF (**2**), position 11 [L-Msa11,D-Trp8]-SRIF (**3**), or position 7 [L-Msa7,D-Trp8]-SRIF (**4**), and [L-Msa7]-SRIF (**5**), were prepared by solid-phase peptide synthesis on 2-chlorotrityl chloride resin, using the Fmoc/tBu strategy. Scheme 1 shows the preparation of [L-Msa6,D-Trp8]-SRIF (**2**). Peptides **3–5** were prepared using the same strategy. When the nonnatural amino acid was coupled, only 1.5 equivalents were used.



**Scheme 1.** a) 1. Fmoc-L-Cys(Trt)-OH (3 equiv), DIEA (3 equiv), 2. MeOH; b) 1. Piperidine 20% DMF, 2. Fmoc-AA-OH (1.5–3 equiv), DIPCDI (3 equiv), HOBT (3 equiv), DMF ( $\times 12$ ), 3. Piperidine 20% DMF, 4. Boc-Ala-OH, DIPCDI, HOBT, DMF; c) 1. CH<sub>2</sub>Cl<sub>2</sub>/TFE/AcOH (7:2:1), 2. I<sub>2</sub>, 3. TFA/CH<sub>2</sub>Cl<sub>2</sub>/anisole/H<sub>2</sub>O (12:7:2:1). Boc = *tert*-butoxycarbonyl, DIEA = diisopropylethylamine, DIPCDI = diisopropylcarbodiimide, DMF = *N,N'*-dimethylformamide, Fmoc = *N*-(9-fluorenylmethoxycarbonyl), HOBT = 1-hydroxybenzotriazole, TFA = trifluoroacetic acid, TFE = 2,2,2-trifluoroethanol

With the purified peptides **2–5** in hand, we first measured the selectivity of each one for each of the five receptors (SSTR1–5) in binding assays using stable CHO (Chinese hamster ovary) cell lines. The efficacy of the interaction

**Table 1:** Affinity of somatostatin, [D-Trp8]-SRIF, octreotide, and peptides 2–5 to receptors SSTR1–5.  $K_i$  values [nM]  $\pm$  SEM.<sup>[a]</sup>

	SSTR1	SSTR2	SSTR3	SSTR4	SSTR5	$t_{1/2}$ [h]
Somatostatin (SRIF)	0.43 $\pm$ 0.08	0.0016 $\pm$ 0.0005	0.53 $\pm$ 0.21	0.74 $\pm$ 0.07	0.23 $\pm$ 0.04	2.75
[D-Trp8]-SRIF	<b>0.32 <math>\pm</math> 0.11</b>	<b>0.001 <math>\pm</math> 0.0007</b>	<b>0.61 <math>\pm</math> 0.02</b>	5.83 $\pm$ 0.44	<b>0.46 <math>\pm</math> 0.24</b>	19.7
Octreotide	300 $\pm$ 85	<b>0.053 <math>\pm</math> 0.011</b>	15.2 $\pm$ 5.9	$> 10^3$	11.53 $\pm$ 1.91	200
[L-Msa6,D-Trp8]-SRIF ( <b>2</b> )	3.08 $\pm$ 0.9	4.55 $\pm$ 0.66	<b>0.78 <math>\pm</math> 0.1</b>	4.70 $\pm$ 0.92	<b>0.36 <math>\pm</math> 0.003</b>	<b>26</b>
[L-Msa11,D-Trp8]-SRIF ( <b>3</b> )	3.35 $\pm$ 1.32	0.14 $\pm$ 0.06	1.31 $\pm$ 0.2	$> 10^3$	<b>0.73 <math>\pm</math> 0.19</b>	<b>41</b>
[L-Msa7,D-Trp8]-SRIF ( <b>4</b> )	<b>0.33 <math>\pm</math> 0.09</b>	<b>0.0024 <math>\pm</math> 0.001</b>	7.49 $\pm$ 0.63	$> 10^3$	$> 10^3$	<b>25</b>
[L-Msa7]-SRIF ( <b>5</b> )	4.17 $\pm$ 1.45	<b>0.019 <math>\pm</math> 0.009</b>	$> 10^3$	28.72 $\pm$ 6.9	$> 10^3$	<b>5.2</b>

[a] Numbers in bold represent data in close proximity to (black) or below (grey) the SRIF values.

against each receptor was assessed in competitive assays using the membranes of the cultured cells and  $^{125}$ I-labeled somatostatin. Somatostatin, [D-Trp8]-SRIF, and octreotide were used as controls (Table 1).

[L-Msa6,D-Trp8]-SRIF (**2**) showed high affinity towards SSTR3 and SSTR5; in fact, its dissociation constants ( $K_i$ ) for these receptors are similar to those of somatostatin, which are 20 to 30 times lower than those of octreotide (Table 1). [L-Msa11,D-Trp8]-SRIF (**3**) exhibited high affinity for SSTR5, and significant affinity (although lower than that of somatostatin) towards SSTR1, SSTR2, and SSTR3 (Table 1).

[L-Msa7,D-Trp8]-SRIF (**4**) showed striking affinity for SSTR2—even higher than that of octreotide. Its inhibition constant for SSTR2 (1.5 times that of natural SRIF) compares very favorably to that of octreotide (33 times lower than that of SRIF). Moreover, **4** showed impressive affinity towards SSTR1, in remarkable contrast to octreotide. Finally [L-Msa7]-SRIF (**5**) which lacks D-Trp8, shows a similar profile than **4** albeit with higher  $K_i$  values (Table 1).

To evaluate the structural effects of these site-directed modifications and subsequently correlate them with the biological activity observed, we used NMR spectroscopy to analyze the conformations of these four peptides in aqueous solution and then compared each one to that of somatostatin. In all cases proton resonance assignments were identified using two-dimensional (2D) TOCSY and NOESY homo-nuclear experiments.<sup>[20a]</sup> Somatostatin, as deduced from the pattern of the NOE data, populates several conformations in solution. All the analogues (**2–5**) showed more intense NOE data than did somatostatin, although the majority of the peaks present in the NMR spectra of these analogues are also detected in the parent compound. This indicates that each analogue is structurally similar to one of the characteristic conformations of the hormone in solution. As shown in the structures below, the side-chain orientation of peptide **2** is very different from that of the remaining peptides, thus explaining why the restraints observed in somatostatin cannot be fitted to a unique conformation.<sup>[12]</sup>

Each of the well-defined two-dimensional spectra of compounds **2–5**, enabled us to characterize their main conformation in solution using the software Crystallography & NMR System (CNS).<sup>[20b]</sup> To generate the list of experimental restraints for the calculation, the volume of all assigned peaks was integrated, and then transformed into distances. Three sets of calculations (120 structures each) were run until the best match between assignments and final structures was obtained. After performing the calculations, all

the obtained structural results were consistent with the NMR data.

We first analyzed the structural effects of replacing Phe6 with Msa. Analysis of the 2D NOESY spectrum of [L-Msa6,D-Trp8]-SRIF (**2**) suggested the presence of a well-defined structure in solution (Figure 3). The dominant conformer of **2**

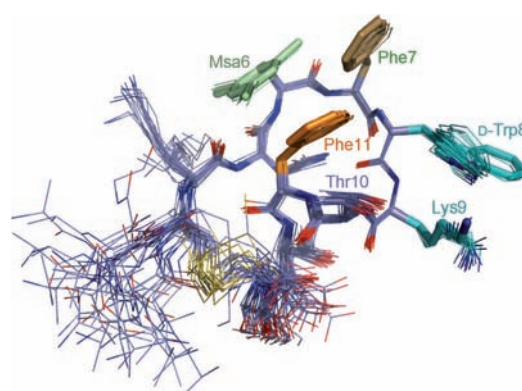


**Figure 3.** Superimposition of 28 minimum-energy conformers of [L-Msa6,D-Trp8]-SRIF (**2**) as calculated based on NMR data using the backbone and the side chains of residues 6 to 11 for the fitting.<sup>[22]</sup>

contains a cluster of three aromatic rings (residues 6, 7, and 11) defined by a large set of NOE interactions among them. As expected, the two aromatic rings of Msa6 and Phe11 are in close proximity because of a strong face-to-face  $\pi$ - $\pi$  interaction.<sup>[21]</sup> Numerous contacts between residues Lys9 and D-Trp8 are also observed in this peptide.

Peptide [L-Msa11,D-Trp8]-SRIF (**3**) is also highly structured. A superimposition of 30 selected low-energy conformers of this peptide reveals that the region containing residues Phe6-Phe7-D-Trp8-Lys9-Thr10-Msa11 is well ordered (root-mean-square deviation (RMSD) value of 0.384 for the backbone; Figure 4). Peptide **3** also exhibited a strong  $\pi$ - $\pi$  interaction between the Phe6 and Msa11 rings, whereby the Phe7 is located on the opposite face of the molecule. The orientation is defined by contacts between the Phe6 ring and the Msa11 ring plus its methyl groups. This aromatic interaction most likely fixes the backbone conformation (a detailed geometric analysis of the  $\pi$ - $\pi$  aromatic interaction is given in the Supporting Information). Interestingly, the  $\pi$ - $\pi$  interaction occurs at the opposite molecular face relative to that observed in analogue **2**. However, the

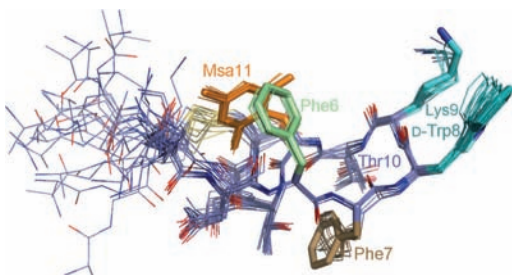


**Figure 4.** The most stable conformers of [L-Msa11, D-Trp8]-SRIF (**3**) as deduced based on NMR data.<sup>[22]</sup>

relative orientation of Lys9 and Trp8 side chains is the same in both compounds.

As predicted, substituting Phe with Msa either in position 6 or 11 afforded highly structured peptides, which feature an internal  $\pi$ - $\pi$  aromatic interaction between the two aromatic residues.<sup>[21]</sup> However, consequences of introducing Msa into the vicinal position 7 were difficult to predict. To this end, we investigated structures (in solution) of [L-Msa7, D-Trp8]-SRIF (**4**) and [L-Msa7]-SRIF (**5**). As deduced from 2D NMR data combined with CNS calculations, peptide **4** showed a well-ordered family of structures showing a hairpin in the region encompassing residues 6 to 11 (Figure 5). This conformation is

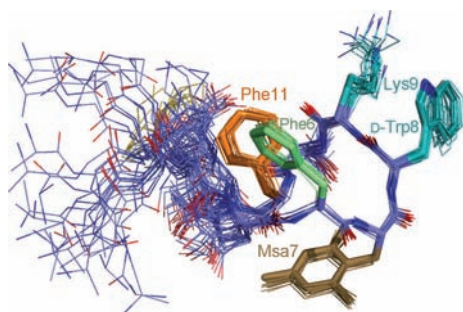


**Figure 5.** Superimposition of the 35 minimum-energy conformers of [L-Msa7, D-Trp8]-SRIF (**4**) that were calculated based on NMR data.<sup>[22]</sup>

defined by contacts between the aromatic rings of Phe6 and of Phe11 and by a set of contacts between the side chains of D-Trp8 and of Lys9; such contacts restrict the hairpin register. Interestingly, peptide **4** is structurally very similar to peptide **3** although in the former the aromatic interaction is distinctly edge-to-face, as defined by contacts between the Phe6 aromatic ring with both Phe11 and the side chain of Lys4. Peptide **5** with Trp8 in its natural configuration was also sufficiently structured to have its 3D structure determined by NMR spectroscopy. The 24 calculated minimum-energy conformers that fit the experimental data are shown in Figure 6. As it seen in the figure, this structure also contains the hairpin, thus indicating that D-Trp8 additionally stabilizes a conformation that already exists in the natural sequence, and it has been suggested to be essential for the biological activity of somatostatin.<sup>[18]</sup> The Trp8-Lys9 interactions are reflected in the upfield shifted  $\gamma$  protons of Lys which are shielded by the aromatic indole ring.



**Figure 6.** Superimposition of the 24 minimum-energy conformers of [L-Msa7]-SRIF (**5**) that were calculated based on NMR data.<sup>[22]</sup> (RMSD value of 0.7 for the backbone).

On the basis of the NMR data that we obtained for each structure, we deduced that the Msa7 residue is not involved in forming  $\pi$ - $\pi$  interactions with either Phe6 or Phe11 since it is located on the opposite face of the molecule. However the position occupied by the aromatic ring at position 7 (below the hairpin, peptides **3**, **4**, and **5**; as shown in Figures 4, 5, and 6, respectively) helps to stabilize the  $\pi$ - $\pi$  interaction between the aromatic rings in positions 6 and 11. To the best of our knowledge, peptides **3–5** are the best structurally defined 14-residue somatostatin analogues described to date. Peptide **4** is the least flexible among these exhibiting the most highly structured conformation because of the combined effects of reinforced aromatic interaction between Phe6 and Phe11 and the presence of D-Trp8 in the structure. (RMSD = 0.3)

During the development of short peptide analogues in the 1990s, the structural rigidity of compounds containing the somatostatin pharmacophore was correlated to their affinity for SSTR2.<sup>[23]</sup> The outstanding affinity of peptide **4** for SSTR2 is in good agreement with its high rigidity. We reasoned that the well-defined conformation that we found for **4** is probably very close to the native conformation of somatostatin when it binds to SSTR2. Moreover, we also hypothesized that the significant activity of peptide **4** against SSTR1 is derived from the  $\pi$ - $\pi$  interaction between Msa7 and the Phe<sup>195</sup> present in SSTR1, according to the pharmacophore proposed by Kaupmann et al.<sup>[24]</sup> In peptide **4**, Msa7 could interact with Phe<sup>195</sup> through a reinforced  $\pi$ - $\pi$  interaction, a scenario that would explain the fact that this analogue showed greater affinity for SSTR1 than the parent compound. Thus, in line with the suggested induced-fit mechanism for SSTR1,<sup>[25]</sup> the enhanced aromatic-aromatic interactions between Msa7 and Phe<sup>195</sup> would be essential for the affinity of **4** (which is much more rigid than peptide **5**) to receptor SSTR1.

Peptide **2** (Msa in position 6) was found to have a completely different selectivity profile than **4**, and it was in good agreement with its distinct 3D structure: it binds SSTR3 and SSTR5 with affinities of the same order of magnitude as that of somatostatin.

In summary, we obtained two conformationally rigid somatostatin analogues with complementary selectivity, and they mimic two of the different conformations that coexist in the native hormone.

Finally, we measured the serum stability of our peptides as well as that of octreotide, somatostatin, and [D-Trp8]-SRIF, for the sake of comparison. Although the half-life of peptides **2–4** in serum is not as high as that of octreotide, these three analogues were on average 10 to 20 times more stable than somatostatin. Their greater stability probably stems from the presence of unnatural amino acids and, very likely, from the stronger interaction between the residues at positions 6 and 11 relative to that in the parent compound. As expected, the half-life of peptide **5** with L-Trp8 is only twice as high as that of somatostatin. The surprisingly the long half-life of analogue **3** (Msa in position 11) relative to peptides **2** and **4**, may corroborate the fact that the unnatural aromatic residue in position 11 shields the residue at position 6, as previously suggested.<sup>[10b]</sup>

To date, the most conformationally restricted somatostatin analogues have been developed by deletion of amino acids, reduction of ring size, or formation of a covalent bridge. These modifications usually improve the intrinsic pharmacological properties associated with peptide drugs. However, we have followed a different approach to obtain analogues with greater rigidity, thus obtaining four new somatostatin analogues with unique activity and selectivity profiles for SSTR1-5, by fine-tuning the electronic and steric properties of specific aromatic residues. We have exploited the noncovalent interactions between the aromatic residues to modulate the conformational flexibility and provide major advantages in receptor selectivity and serum stability. By enhancing aromatic–aromatic interactions in somatostatin analogues, we have obtained four peptides with high receptor selectivity and with restricted conformations that enabled us to determine their 3D structures by NMR spectroscopy. Furthermore, we have elucidated the key aspects of the selectivity against the five somatostatin receptors by simply introducing an unnatural Msa amino acid in the original sequence. Our results prove that the modification of noncovalent interactions is a promising strategy in drug discovery and opens new possibilities for designing unprecedented peptide analogues of natural compounds.

## Experimental Section

**NMR assignment and structure calculation:** NMR data were acquired at 285 K, using trifluoroacetate as a counter-ion at a pH 4.5 on a Bruker Avance III 600 MHz spectrometer equipped with a  $z$ -pulse field gradient unit. All spectra were processed with NMRPipe/NMRDraw software<sup>[26a]</sup> and were analyzed with CARA.<sup>[26b]</sup> The volume of all manually assigned peaks in the NOESY spectrum was integrated to generate the list of experimental restraints. The structures were water refined and ranked based on minimum values of energy-terms and violations of the experimental restraints. Molecular images were generated using PyMOL.

**Receptor–ligand binding assay.** All receptor binding assays were performed with membranes isolated from CHO-K1 cells expressing human SRIF-14 receptor.<sup>[27a]</sup> IC<sub>50</sub> values were calculated using a curve-fitting program (GraphPad Prism). The K<sub>i</sub> values for the compounds were determined as previously described.<sup>[27b]</sup> Data represent the mean  $\pm$  SEM of values from at least three separate experiments, each of which was performed in triplicate.

Received: September 9, 2011

Published online: December 9, 2011

**Keywords:** conformation analysis · NMR spectroscopy · noncovalent interactions · peptides · drug design

- [1] W. Saenger, *Principal of Nucleic Acid Structure*, Springer, New York, **1984**.
- [2] a) U. Skögl, M. Vihinen, L. Nilsson, P. Liljeström, *Structure* **1996**, *4*, 519–529; b) M. Ma, Y. Kuang, Y. Gao, Y. Zhang, P. Gao, B. Xu, *J. Am. Chem. Soc.* **2010**, *132*, 2719–2728; c) C. A. Hunter, *J. Chem. Soc. Chem. Commun.* **1991**, 749–751.
- [3] a) S. K. Burley, G. A. Petsko, *Science* **1985**, *229*, 23–28; b) T. Blundell, J. Singh, J. Thornton, S. K. Burley, G. A. Petsko, *Science* **1986**, *234*, 1005–1005; c) J. Singh, J. M. Thornton, *FEBS Lett.* **1985**, *191*, 1–6.
- [4] R. Mahalakshmi, S. Raghothama, P. Balaram, *J. Am. Chem. Soc.* **2006**, *128*, 1125–1138.
- [5] a) M. J. Macias, S. Wiesner, M. Sudol, *FEBS Lett.* **2002**, *513*, 30–37; b) A. Laederach, A. H. Andreotti, D. B. Fulton, *Biochemistry* **2002**, *41*, 12359–12368.
- [6] a) P. Brazeau, W. Vale, R. Burgus, N. Ling, M. Butcher, J. Rivier, R. Guillemin, *Science* **1973**, *179*, 77–79; b) R. Burgus, N. Ling, M. Butcher, R. Guillemin, *Proc. Natl. Acad. Sci. USA* **1973**, *70*, 684–688.
- [7] a) G. Garcia-Tsao, A. J. Sanyal, N. D. Grace, W. Carey, *Hepatology* **2007**, *46*, 922–938; b) J. Ayuk, M. C. Sheppard, *Postgrad. Med. J.* **2006**, *82*, 24–30; c) M. Pawlikowski, G. Melen-Mucha, *Curr. Opin. Pharmacol.* **2004**, *4*, 608–613; d) W. W. de Herder, L. J. Hofland, A. J. van der Lely, S. W. J. Lamberts, *Endocr.-Relat. Cancer* **2003**, *10*, 451–458.
- [8] a) D. Hoyer, G. I. Bell, M. Berelowitz, J. Epelbaum, W. Feniuk, P. P. A. Humphrey, A. O'Carroll, Y. C. Patel, A. Schonbrunn et al., *Trends Pharmacol. Sci.* **1995**, *16*, 86–88; b) Y. C. Patel, C. B. Srikant, *Endocrinology* **1994**, *135*, 2814–2817.
- [9] D. F. Veber, F. W. Holly, W. J. Paleveda, R. F. Nutt, S. J. Bergstrand, M. Torchiana, M. S. Glitzer, R. Saperstein, R. Hirschmann, *Proc. Natl. Acad. Sci. USA* **1978**, *75*, 2636–2640.
- [10] a) B. H. Arison, R. Hirschmann, W. J. Paleveda, S. F. Brady, D. F. Veber, *Biochem. Biophys. Res. Commun.* **1981**, *100*, 1148–1153; b) S. Neelamkavil, B. Arison, E. Birzin, J. Feng, K. Chen, A. Lin, F. Cheng, L. Taylor, E. R. Thornton, A. B. Smith III, R. Hirschmann, *J. Med. Chem.* **2005**, *48*, 4025–4030.
- [11] a) A. Jans, K. Hallenga, G. Van Binst, A. Michel, A. Scarso, J. Zanen, *Biochim. Biophys. Acta Protein Struct. Mol. Enzymol.* **1985**, *827*, 447–452; b) E. M. M. Van den Berg, A. W. H. Jans, G. Van Binst, *Biopolymers* **1986**, *25*, 1895–1908.
- [12] a) B. H. Arison, R. Hirschmann, D. F. Veber, *Bioorg. Chem.* **1978**, *7*, 447–451; b) M. Knappenberg, A. Michel, A. Scarso, J. Brison, J. Zanen, K. Hallenga, P. Deschrijver, G. Van Binst, *Biochim. Biophys. Acta Protein Struct. Mol. Enzymol.* **1982**, *700*, 229–246; c) L. A. Buffington, V. Garsky, J. Rivier, W. A. Gibbons, *Biophys. J.* **1983**, *41*, 299–304.
- [13] a) K. Gademann, M. Ernst, D. Hoyer, D. Seebach, *Angew. Chem.* **1999**, *111*, 1302–1304; *Angew. Chem. Int. Ed.* **1999**, *38*, 1223–1226; b) C. R. R. Grace, J. Erchegeyi, S. C. Koerber, J. C. Reubi, J. Rivier, R. Riek, *J. Med. Chem.* **2006**, *49*, 4487–4496; c) E. Biron, J. Chatterjee, O. Ovadia, D. Langenegger, J. Brueggen, D. Hoyer, H. A. Schmid, R. Jelnick, C. Gilon, A. Hoffman, H. Kessler, *Angew. Chem.* **2008**, *120*, 2633–2637; *Angew. Chem. Int. Ed.* **2008**, *47*, 2595–2599; d) J. M. Beierle, W. S. Horne, J. H. van Maarseveen, B. Waser, J. C. Reubi, M. R. Ghadiri, *Angew. Chem.* **2009**, *121*, 4819–4823; *Angew. Chem. Int. Ed.* **2009**, *48*, 4725–4729; e) J. Erchegeyi, R. Cescato, B.

- Waser, J. E. Rivier, J. C. Reubi, *J. Med. Chem.* **2011**, *54*, 5981–5987.
- [14] W. Bauer, U. Briner, W. Doepfner, R. Haller, R. Huguenin, P. Marbach, T. J. Petcher, J. Pless, *Life Sci.* **1982**, *31*, 1133–1140.
- [15] W. Vale, J. Rivier, N. Ling, M. Brown, *Metab. Clin. Exp.* **1978**, *27*, 1391–1401.
- [16] R. Ramón, P. Martín-Gago, X. Verdager, M. J. Macias, P. Martín-Malpartida, J. Fernández-Carneado, M. Gomez-Caminals, B. Ponsati, P. López-Ruiz, M. A. Cortés, B. Colás, A. Riera, *ChemBioChem* **2011**, *12*, 625–632.
- [17] E. Medina, A. Moyano, M. A. Pericas, A. Riera, *Helv. Chim. Acta* **2000**, *83*, 972.
- [18] a) J. Rivier, M. Brown, W. Vale, *Biochem. Biophys. Res. Commun.* **1975**, *65*, 746–751; b) B. H. Arison, R. Hirschmann, D. F. Veber, *Bioorg. Chem.* **1978**, *7*, 447–451; c) O. Ovadia, S. Greenberg, B. Laufer, C. Gilon, A. Hoffman, H. Kessler, *Expert Opin. Drug Discovery* **2010**, *5*, 655–671.
- [19] R. Ramón, M. Alonso, A. Riera, *Tetrahedron: Asymmetry* **2007**, *18*, 2797–2802.
- [20] a) K. Wüthrich, G. Wider, G. Wagner, W. Braun, *J. Mol. Biol.* **1982**, *155*, 311–319; b) A. T. Brünger, P. D. Adams, G. M. Clore, W. L. DeLano, P. Gros, R. W. Grosse-Kunstleve, J. S. Jiang, J. Kuszewski, M. Nilges, N. S. Pannu, R. J. Read, L. M. Rice, T. Simonson, G. L. Warren, *Acta Crystallogr. Sect. D* **1998**, *54*, 905–921.
- [21] The topology of the mesityl precludes the mesityl alanine playing the “edge” role in an edge-to-face interaction.
- [22] The side chains of Trp8 and of Lys9 are depicted in cyan, and the disulfide bridge, in gold. The side chains of residues 6, 7, and 11 are shown in light green, brown, and orange, respectively and are labeled for clarity. More detailed structural data for each peptide, including a text file with the 35 low-energy conformers in PDB format, are provided in the Supporting Information.
- [23] T. Reisine, *Cell. Mol. Neurobiol.* **1995**, *15*, 597–614.
- [24] K. Kaupmann, C. Bruns, F. Raulf, H. P. Weber, H. Mattes, H. Lubbert, *EMBO J.* **1995**, *14*, 727–735.
- [25] J. Erchegeyi, R. Cescato, C. R. R. Grace, B. Waser, V. Piccand, D. Hoyer, R. Riek, J. E. Rivier, J. C. Reubi, *J. Med. Chem.* **2009**, *52*, 2733–2746.
- [26] a) F. Delaglio, S. Grzesiek, G. Vuister, G. Zhu, J. Pfeifer, A. Bax, *J. Biomol. NMR* **1995**, *6*, 277–293; b) R. Keller, *The Computer Aided Resonance Assignment Tutorial*, 1st ed., CANTINA Verlag, **2004**.
- [27] a) S. Rens-Domiano, S. F. Law, Y. Yamada, S. Seino, G. I. Bell, T. Reisine, *Mol. Pharmacol.* **1992**, *42*, 28–34; b) Y.-C. Cheng, W. H. Prusoff, *Biochem. Pharmacol.* **1973**, *22*, 3099–3108.